

UCLA

UCLA Previously Published Works

Title

Interaction and breakup of inwardly rotating spiral waves in an inhomogeneous oscillatory medium

Permalink

<https://escholarship.org/uc/item/79j20404>

Journal

Physical Review E, 75(1)

ISSN

1539-3755

Authors

Xie, Fagen
Weiss, James N

Publication Date

2007

Peer reviewed

Interaction and breakup of inwardly rotating spiral waves in an inhomogeneous oscillatory medium

Fagen Xie¹ and James N. Weiss²

¹Research Department, Kaiser Permanente, 100 S. Los Robles Ave, Pasadena, California 91101, USA

²Departments of Medicine (Cardiology) and Physiology, UCLA Cardiovascular Research Laboratory, David Geffen School of Medicine at UCLA, Los Angeles, California 90095, USA

(Received 2 October 2006; published 23 January 2007)

We studied the effects of spatial inhomogeneities on inwardly rotating spiral waves in a typical type of oscillatory medium using the complex-Ginzburg-Landau equation. With a small degree of the inhomogeneity in the medium, the slower inward spiral always suppressed a faster spiral; when the inhomogeneity exceeded a critical value, however, a transition occurred to the coexistence of multiple inward spirals, insulated by regions of highly disordered wave break. The occurrence of this transition is examined theoretically and shown to be due to the Eckhaus instability.

DOI: [10.1103/PhysRevE.75.016107](https://doi.org/10.1103/PhysRevE.75.016107)

PACS number(s): 82.40.Ck, 05.45.-a

I. INTRODUCTION

Spiral waves have been extensively investigated in a variety of spatial systems, including chemical and biological systems [1]. Usually, spiral waves in excitable systems rotate outwardly from the spiral core area, but in oscillatory systems, they can rotate outwardly or inwardly depending on the sign of the phase velocity in the system. Spiral wave rotates outwardly for positive phase velocity, and vice versa for negative phase velocity [2–6]. Most studies of inward spiral waves in oscillatory systems have focused on spatially homogenous media [2–6]. However, real systems are commonly spatially inhomogeneous. The effects of inhomogeneity on outwardly rotating spiral waves in excitable and oscillatory systems have been extensively examined theoretically [7–10] and experimentally [11]. In these studies, weak inhomogeneity leads to collision and annihilation of spirals with different frequencies, such that the fastest spiral finally suppresses all slower spirals [7–11]. If the inhomogeneity becomes large enough, however, multiple spirals with different frequencies can coexist [9,10]. It is not known whether inhomogeneity has the same effects on inward spiral waves as outward spiral waves. A recent interesting study [8] showed that in a two-dimensional medium of a complex Ginzburg-Landau equation, weak inhomogeneity caused the lower frequency spiral to suppress the spiral with higher frequency in the parameter regime $\beta < \alpha$ and $\alpha > 0$. The theoretical analysis of CGLE [3–5] revealed that the spirals in this parameter regime rotated inwardly. However, to our knowledge, there is no information about the effects of strong inhomogeneity on the dynamics of inward spiral waves, and whether the breakup of inward spirals can be produced by inhomogeneity, and, if so, what mechanism is involved. In this paper, we focused our investigations on this problem in a typical oscillatory system—the two-dimensional complex Ginzburg-Landau equation (CGLE). In the next section, we present the mathematical model and the numerical simulations in this system. The theoretical analysis of the Eckhaus instability in the presence of large inhomogeneities is presented in Sec. III. The paper ends with the conclusions and discussions of the results.

II. MATHEMATICAL MODEL AND NUMERICAL RESULTS

The CGLE provides a universal description of extended systems in the vicinity of a supercritical Hopf bifurcation [12], as described by the following reaction-diffusion equation

$$\partial W / \partial t = W - (1 + i\alpha)W|W|^2 + (1 + i\beta)\nabla^2 W, \quad (1)$$

in which α and β are control parameters. Analytical analysis of the entire parameter (α, β) space [3–5] showed that outwardly rotating spiral waves can form in a homogenous medium in some parameter regions while the spiral waves rotate inwardly in the other regions (see [5] for specific details). Throughout this paper, we fixed $\beta=0.3$ and varied α , keeping $\alpha < 0$ so that the spiral waves rotated inwardly [5,6]. In order to create an inhomogeneous medium, we modified the parameter α as a function of space. Although in real systems [11], the inhomogeneity could be very complex, to study the interaction of two different inward spiral waves systematically, we introduced the following simple inhomogeneity between the two halves of the medium.

$$\alpha = \begin{cases} \alpha_L, & x \leq L_x/2, & 0 \leq y \leq L_y, \\ \alpha_R, & L_x/2 < x \leq L_x, & 0 \leq y \leq L_y. \end{cases} \quad (2)$$

As $\alpha_L = \alpha_R$, the system describes a homogeneous medium. Without losing generality, we set $\alpha_L \geq \alpha_R$, so that the inward spiral on the left side of the medium always rotated more slowly than the right-sided inward spiral. Equation (1) was simulated in a two-dimensional (2D) square sheet with the system size $L_x = L_y = 100$ for the homogenous condition, and a 2D rectangular sheet with $L_x = 200, L_y = 100$ for the inhomogeneous condition. No-flux boundary conditions and discretization of $dx = dy = 0.5$ and $dt = 0.01$ were used in an explicit Euler-scheme. The spiral wave in the homogeneous medium was initiated by using the limit cycle obtained from the local dynamics of Eq. (1), while the initiated spiral wave in inhomogeneous medium was constructed from the final stable spiral waves in the corresponding homogenous case.

We found that the dynamical behavior of the inward spiral wave in the homogenous case ($\alpha_L = \alpha_R = \alpha$) qualitatively

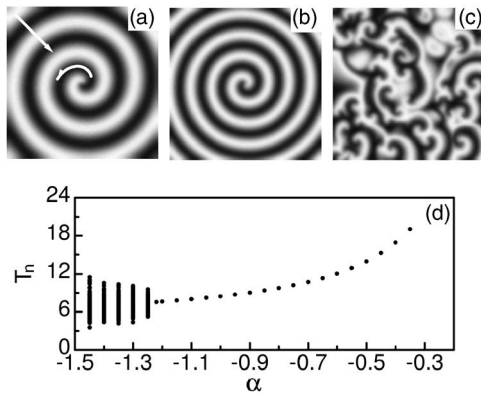


FIG. 1. (a)–(c) The snapshots of $\text{Re}(W)$ in Eq. (1) in a homogeneous medium ($L_x=L_y=100$), for $\beta=0.3$ and different α , after the transient. The black to white gray scale represents the lowest value (-1.0) to the highest value (1.0). The white arrows indicate the direction of wave propagation. (a) $\alpha=-0.60$; (b) $\alpha=-1.00$; (c) $\alpha=-1.30$; (d) The corresponding bifurcation diagram of the steady state rotation period of inward spiral waves versus α .

changed as the control parameter α decreased from zero. For small absolute values of α , the inward spiral wave was completely stable after a transient process. The snapshots of $\text{Re}(W)$ for $\alpha=-0.60$ and -1.00 are shown in Figs. 1(a) and 1(b), respectively. These stable spiral waves propagated from the boundary of the medium to the spiral core center, as shown by the white arrows. As α was decreased to a critical value $\alpha \approx -1.25$, the inward spiral wave became unstable and broke into a complex multiple spirals state as shown in Fig. 1(c) for $\alpha=-1.30$. The transition is clearly shown by the rotation period plots of the inward spiral in Fig. 1(d), where the spiral rotation periods were irregular for $\alpha < -1.25$ but regular for $\alpha > -1.25$.

To investigate whether inhomogeneity could produce qualitative changes in the dynamics of inward spiral waves, we limited both α_L and α_R to the stable regime ($\alpha > -1.25$). We fixed $\alpha_L = -0.60$ to produce a slower inward spiral on the left-side of the medium, and then altered α_R with respect to this value of α_L to produce a faster inward spiral on the right side of the medium. The interaction between the two inward spiral waves initiated in the left and right halves of the medium strongly depended on the degree of the inhomogeneity $\Delta\alpha = \alpha_L - \alpha_R$. For α_R greater than a critical value α_R^c of ≈ -0.92 , the wave front of the left-sided slower inward spiral gradually invaded the domain of the right-sided faster inward spiral, until the faster spiral was swept away. Figure 2(a) shows the interaction of the two inward spiral waves in the medium for $\alpha_R = -0.80$. It is interesting to note that the interaction of inward spirals is essentially the inverse of that which occurs between outward spirals. In the case of outward spirals, the wave fronts from the faster spiral arrive sooner at the interface zone and progressively invade the domain of the slower spiral, until the faster outward spiral sweeps the slower spiral off the border of the medium [7–11]. With inward spirals, however, the wave fronts propagate towards the center of the spiral (white arrows). Thus, wave fronts from the faster spiral recede more rapidly from the interface zone than wave fronts from the slower spiral,

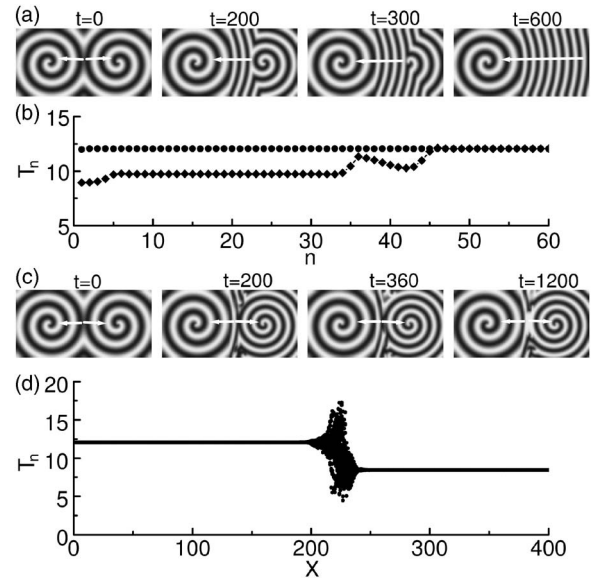


FIG. 2. (a) Evolution of interacting inward spiral waves in an inhomogeneous medium ($L_x=200, L_y=100$) for $\beta=0.3$, $\alpha_L=-0.60$ (left half of medium) and $\alpha_R=-0.80$ (right half). The white arrows indicate the direction of wave propagation. The right-sided inward spiral with faster frequency is gradually unwound by the left-sided inward spiral with the slower frequency, and pushed off the boundary. (b) The corresponding rotation periods of spirals in (a) versus the beat number at location $x=75.0, y=50.0$ in the left-sided α_L region (solid dots) and location $x=175.0, y=50.0$ in the right-sided α_R region (diamonds). (c) Same as (a), except $\alpha_L=-1.00$. Note the two inward spirals with different frequencies coexist, due to the insulating effects of wave breaks in the middle region. (d) The corresponding steady state rotation periods in (c) versus distance along x at $y=50.0$.

allowing the slower inward spiral wave to invade progressively the faster inward spiral wave’s domain. The rotation periods measured from the left ($x=75.0, y=50.0$) and right sides ($x=175.0, y=50.0$) of the medium versus the beat number are shown in Fig. 2(b) by the solid dots and the diamonds, respectively. The rotation period in the left side of the medium was always constant, while the rotation period in the right side was initially constant, corresponding to the rotation period of the faster inward spiral. As the wave fronts from the slower left-sided spiral penetrated the core region of the faster right-sided inward spiral, however, the rotation speed decreased, and subsequently synchronized to the rotation period of the slowest inward spiral wave.

When α_R was beyond α_R^c , however, the interaction between the two inward spiral waves changed qualitatively. Wave propagation from the right side of the midline towards the slower left-sided inward spiral core center became unstable and broke up into complex disordered multiple wavelets. This occurred because once the left-sided inward spiral captured tissue on the right side, the frequency of these waves was too fast for them to propagate leftward with 1:1 conduction across the middle towards the core of the left-sided inward spiral. Meanwhile, while the distal wave fronts of the faster right-sided inward spiral continued to propagate stably towards their core. Thus, the wave breakup in the right

midline region protected the core of the faster right-sided inward spiral from being unwound and swept away, allowing two inward spirals with different frequencies to coexist. Figure 2(c) shows snapshots of the interactions between the two spirals when $\alpha_R = -1.00$, and Fig. 2(d) shows the corresponding rotation periods along the x space at $y = 50.0$. The inward spirals in the left and right sides of the medium rotated stably with unique rotating periods, while wave breaks in the right midline zone separating them were highly disordered.

Generally, the critical value α_R^c depends on the value of α_L . Regardless of the α_L value, when $\alpha_R > \alpha_R^c$, the interaction between the slower left-sided inward spiral (named SPL) and the faster right-sided inward spiral (named SPR) can be separated into two phases, an invading process and a sweeping process. Figures 3(a) and 3(b) show the evolution of the tip position y and x of the SPR for $\alpha_L = -0.60$ and $\alpha_R = -0.80$, respectively. Initially, the right-sided faster spiral wave rotated periodically around the core center $x = 150.0$, $y = 50$ for nearly 300 times the unit duration, and then it began to drift due to the push from the wave fronts of the left-sided spiral wave. Finally, the right-sided spiral terminated at the lower-right boundary of the medium after 550 times unit duration. Applying the phase matching between the wave fronts between the left-sided spiral with frequency ω_L and the right-sided spiral with frequency ω_R [8], the invading velocity of the one spiral unwinding the other is

$$V = \left| \frac{\omega_R - \omega_L}{k_R + k_L^R} \right|, \quad (3)$$

and the sweeping velocity at which the faster right-sided spiral is swept away is

$$V = \left| \frac{\omega_R - \omega_L}{k_L^R} \right|, \quad (4)$$

where k_R is the wave number of the right-sided spiral, and k_L^R is the wave number of the wave from the left-sided spiral invading into the right-sided region [10]. Both the invading velocity of Eq. (3) and the sweeping velocity of Eq. (4) are identical to the corresponding relationships for outwardly rotating spirals, as previously shown in the theoretical models [8,10] and experimental study [11]. Neglecting curvature effect, for the inhomogeneous condition of Eq. (2), both wave numbers k_L^R and k_R approximately satisfy the following dispersion relation [13]:

$$\omega_L = \alpha_R + (\beta - \alpha_R)(k_L^R)^2, \quad \omega_R = \alpha_R + (\beta - \alpha_R)k_R^2. \quad (5)$$

Note that the wave number k_L^R is different from the wave number k_L of the left-side spiral wave in the left region of the medium, which satisfies the dispersion relation $\omega_L = \alpha_L + (\beta - \alpha_L)k_L^2$ [10]. In weakly inhomogeneous media [8], however, k_L^R is approximately the same as k_L . The theoretical predictions of the invading velocity and the sweeping velocity versus α_R are shown in Figs. 3(c) and 3(d) by the solid line, respectively. The diamonds in Figs. 3(c) and 3(d) are the velocities measured directly from the numerical simulations. The theoretical values agree well with the numerical results.

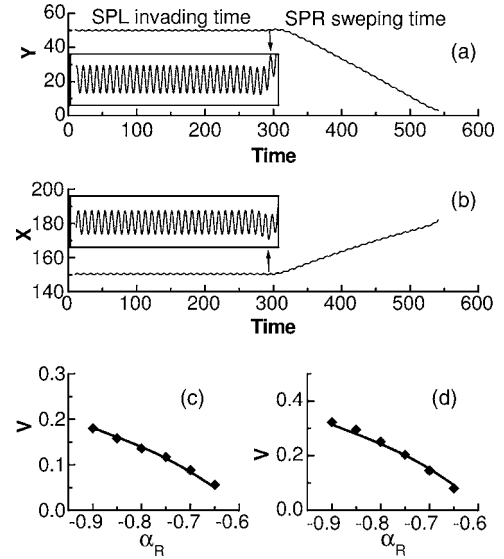


FIG. 3. (a)–(b) The tip position of the faster right-sided inward spiral along the y coordinate (a) and the x coordinate (b) versus time for $\beta = 0.3$, $\alpha_L = -0.60$, and $\alpha_R = -0.80$. Insets show enlargements of the tip positions during the invading process by the slower inward spiral (SPL). (c) The theoretical invading velocity of the slower inward spiral (SPL) from Eq. (3) versus α_R for $\alpha_L = -0.60$ and $\beta = 0.3$. (d) The theoretical sweeping velocity of the faster inward spiral (SPR) from Eq. (4) versus α_R . The theoretical values agree well with the velocities measured directly from numerical simulations [diamonds in (c) and (d)].

III. THE ANALYSIS OF ECKHAUS INSTABILITY AND MECHANISM OF COEXISTENCE OF MULTIPLE INWARD SPIRALS IN THE PRESENCE OF LARGE INHOMOGENEITIES

When α_R is beyond the threshold α_R^c , waves can propagate continuously from the middle region to the spiral core center on the right side, but the slower propagation of the wave from the middle right-side zone towards the core of the slower left-sided spiral wave is not sustained, it breaks up into multiple wavelets due to the absolute Eckhaus instability [6,13–16]. Specifically, since the left-propagated waves are several wavelengths from the left spiral core center, they can be approximately as planar waves, which have the following form:

$$W = F \exp[i(kr - \omega t)],$$

$$\omega = \alpha + (\beta - \alpha)k^2, \quad (6)$$

where $F = \sqrt{1 - k^2}$, and $k^2 < 1$.

Applying the standard wave stability analysis to Eq. (6) [13–15], the criteria of the long-wavelength stability of the planar waves of Eq. (6) is (see Ref. [13] for the detailed calculations)

$$1 + \alpha\beta - 2(1 + \alpha^2)k^2/(1 - k^2) = 0, \quad (7)$$

which is called the Eckhaus instability. This leads to

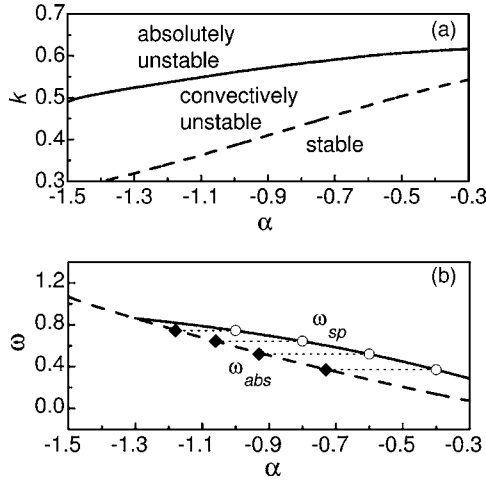


FIG. 4. (a) The threshold of wave numbers for the Eckhaus convective instability (dashed line) and absolute instability (solid line) vs α for $\beta=0.3$. (b) The wave frequency at the onset of the Eckhaus absolute instability (dashed line), and the rotating frequency of the inward spiral wave (solid line) versus α for $\beta=0.3$. The diamonds represent the corresponding α_R threshold for the onset of wave breakup in the medium obtained by numerical simulation at different fixed α_L (open circles) in the left side of the medium.

$$k_c = \sqrt{(1 + \alpha\beta)/(3 + \alpha\beta + 2\alpha^2)}. \quad (8)$$

Thus, all planar or traveling waves with $k < k_c$ are stable and vice versa for those with $k > k_c$. The critical wave number k_c versus α for $\beta=0.3$ is shown in Fig. 4(a) by the dashed line. The area under this dashed line is *Eckhaus stable*. As $k > k_c$, the planar waves become destabilized via the Eckhaus instability. However, the instability can be convective or absolute [13]. Previous studies [6,13–16] showed the breakup of planar waves and spiral (inward or outward) waves in the oscillatory medium was caused by the absolute Eckhaus instability. Applying a small localized longitudinal perturbation $\exp(\pm iqr)$ with $q \parallel k$ to Eq. (6), we obtain the following criteria for the absolute instability (see Ref. [13] for more details)

$$\begin{aligned} \lambda(q) &= -q^2 - F^2 - 2i\beta kq \\ &\quad \pm \sqrt{(1 + \alpha^2)F^4 - (\beta q^2 - 2ikq + \alpha F^2)^2}, \\ \text{Re}[\lambda(q)] &= 0, \\ \partial\lambda/\partial q|_{q_0} &= 0. \end{aligned} \quad (9)$$

where q_0 is the largest saddle point in the complex q plane. The threshold of k for the absolute instability determined by Eq. (9) versus α when $\beta=0.3$ is shown in Fig. 4(a) as the solid line. The area above the solid line is *absolutely unstable*, while the area between the solid and dashed lines is *convectively unstable*. Using the dispersion relation from Eq. (6), the corresponding sustained wave frequency ω_{abs} at the onset of the absolute instability in the medium can be obtained and is shown in Fig. 4(b) as the dashed line. The solid

line in Fig. 4(b) represents the rotating frequency of the inward spiral wave measured in the homogeneous medium. The solid line meets the dashed line at $\alpha \approx -1.27$, which is the threshold for the onset of the inward spiral wave breakup in the homogeneous medium. The threshold is close to the value -1.25 obtained directly from the numerical simulation, as shown in Fig. 1. For the inhomogeneous condition of Eq. (2), wave breaks can be qualitatively described as follows. First, since α_L was fixed in the left-sided region, the corresponding rotating frequency ω_L of the inward spiral wave in this region was also constant. Second, as α_R varied from the initial value α_L , the frequency of the waves in the right side propagating towards the left-sided spiral core center always had the same frequency ω_L of the slower left-sided spiral wave. Therefore, for a fixed α_L in the left-sided region, the critical value of α_R for the onset of the wave breakup in the right-side region is determined by

$$\omega_{abs}(\alpha_R) = \omega_L. \quad (10)$$

The predicted values by Eq. (10) agreed well with these critical values of α_R obtained from the numerical simulations as shown in Fig. 4(b) by the diamonds for four sets of $\alpha_L = -0.40, -0.60, -0.80, -1.0$ (open circles), respectively.

IV. CONCLUSIONS

We have investigated the effects of inhomogeneity on the interaction and the breakup of inward spiral waves in the CGLE system. The occurrence of wave breakup produced by inhomogeneity was theoretically analyzed by examining the absolute Eckhaus instability. The effect of inhomogeneity was strongly dependent on the degree of the inhomogeneity in the medium. First, for small degrees of inhomogeneity, and below a critical value, the interaction between two stable inward spirals resulted in the slower spiral always suppressing the faster one. This is the opposite of the interaction between two stable outward spirals, where the faster spiral wave always suppress the slower one [7–11]. This is because the wave fronts of the faster inward spirals recede towards the core center, while the outward spiral waves propagate out from the core center. However, the invading velocity of the dominated inwardly rotating spiral and the sweeping velocity of the unwound inwardly rotating spiral obeyed the same principles as outwardly rotating spirals found in the theoretical models [8,10] and experimental study [11]. Second, when the degree of inhomogeneity is beyond the critical threshold, wave propagation in the faster spiral region breaks up distant from the core due to the onset of the absolute Eckhaus instability. In this setting, the slower and faster inward spirals become insulated from one another by the region of wave breaks between them, and can coexist. Finally, although the inhomogeneity of Eq. (2) in this study is simple with just two different regions, our findings, especially, the coexistence of multiple inward spirals with different rotating frequencies, are also applicable to more complex inhomogeneous oscillatory media, and can be tested experimentally in real oscillatory systems, such as the BZ-AOT systems [2,11] in similar settings.

- [1] A. T. Winfree, *When Time Breaks Down* (Princeton University Press, Princeton, 1987); *Chemical Waves and Patterns*, edited by R. Kapral and K. Showalter (Kluwer, Dordrecht, 1995); J. Murray, *Mathematical Biology* (Springer, Berlin, 1989).
- [2] V. K. Vanag and I. R. Epstein, *Science* **294**, 835 (2001); *Phys. Rev. Lett.* **87**, 228301 (2001); V. K. Vanag and I. R. Epstein, *ibid.* **88**, 088303 (2002).
- [3] Y. Gong and D. J. Christini, *Phys. Rev. Lett.* **90**, 088302 (2003).
- [4] L. Bruschi, E. M. Nicola, and M. Bär, *Phys. Rev. Lett.* **92**, 089801 (2004).
- [5] E. M. Nicola, L. Bruschi, and M. Bär, *J. Phys. Chem. B* **108**, 14733 (2004).
- [6] F. Xie, D. Xie, and J. N. Weiss, *Phys. Rev. E* **74**, 026107 (2006).
- [7] M. Vinson, *Physica D* **116**, 313 (1998).
- [8] M. Hendrey, E. Ott, and T. M. Antonsen Jr., *Phys. Rev. Lett.* **82**, 859 (1999); *Phys. Rev. E* **61**, 4943 (2000).
- [9] F. Xie, Z. Qu, J. N. Weiss, and A. Garfinkel, *Phys. Rev. E* **59**, 2203 (1999); F. Xie, Z. Qu, J. N. Weiss, and A. Garfinkel, *ibid.* **63**, 031905 (2001).
- [10] M. Zhan, X. Wang, X. Gong, and C. H. Lai, *Phys. Rev. E* **71**, 036212 (2005).
- [11] L. B. Smolka, B. Marts, and A. L. Lin, *Phys. Rev. E* **72**, 056205 (2005).
- [12] *Chemical Oscillations, Waves, and Turbulence*, edited by Y. Kuramoto (Springer, Verlag, 1984).
- [13] I. S. Aranson, L. Aranson, L. Kramer, and A. Weber, *Phys. Rev. A* **46**, R2992 (1992).
- [14] M. Ipsen, L. Kramer, and P. G. Sorensen, *Phys. Rep.* **337**, 193 (2000).
- [15] I. S. Aranson and K. Kramer, *Rev. Mod. Phys.* **74**, 99 (2002).
- [16] M. Bär and M. Or-Guil, *Phys. Rev. Lett.* **82**, 1160 (1999).